

Extended Walfisch-Bertoni Propagation Model to cover Short Range and Millimeter-wave bands

Wataru Yamada¹, Motoharu Sasaki¹, and Naoki Kita¹

¹NTT Corporation

November 22, 2022

Abstract

Extending the frequency range of the Walfisch-Bertoni (W-B) model, which is a representative theoretical model, was investigated. To extend the W-B model, three changes to the original W-B model were made: (i) re-modeling over rooftop path, (ii) introducing a slant path, and (iii) modeling of multiple reflections between buildings. To validate the proposed model, propagation loss predicted by the model was compared with measurement data. The results of the comparison show that propagation loss predicted by the proposed model agrees well with the measurement results.

Extended Walfisch-Bertoni Propagation Model to cover Short Range and Millimeter-wave bands

W. Yamada¹, M. Sasaki¹, and N. Kita¹

¹NTT Access Network Service Systems Laboratories, NTT Corporation.

Abstract

Extending the frequency range of the Walfisch-Bertoni (W-B) model, which is a representative theoretical model, was investigated. To extend the W-B model, three changes to the original W-B model were made: (i) re-modeling over rooftop path, (ii) introducing a slant path, and (iii) modeling of multiple reflections between buildings. To validate the proposed model, propagation loss predicted by the model was compared with measurement data. The results of the comparison show that propagation loss predicted by the proposed model agrees well with the measurement results.

Index terms – millimeter wave, short range, propagation model, propagation loss, 5G, Beyond 5G, 6G

1 Introduction

The fifth-generation mobile communication system (5G) was commercialized in 2020. The main features of 5G are threefold: “enhanced mobile broadband” (eMBB), “massive machine-type communication” (mMTC), and “ultra-reliable low-latency communications” (URLLC) [ITU-RM2410, 2017]. So far, 5G has mainly been operated on sub-6-GHz bands. However, to fully utilize the features of 5G, new frequency bands must be assigned to International Mobile Telecommunications (IMT) systems. Therefore, over the last decade, efforts have been made to develop new frequency bands for IMT systems. As a result, at the World Radiocommunication Conference 2019, a total of 17.25 GHz of new bandwidth from 24.25 to 71 GHz was identified for IMT systems [WRC, 2020]. Moreover, studies on beyond 5G and 6G have begun, and plans to use frequencies up to 300 GHz for IMT have been made [DOCOMO, 2020][Latva-aho et al., 2019]. Unlike radio waves in conventional frequency bands, those in these high-frequency bands have strong straightness.

Several methods for predicting propagation characteristics in high-frequency bands have been developed [Sasaki et al., 2015] [ITUM2412, 2017] [Salous et al., 2020]. These methods mainly use statistical models based on measurement results. Since the statistical models are constructed from measurement data, they have sufficient reliability, but their effectiveness outside the measured frequency range is extremely limited. On the contrary, since a theoretical model is derived from electromagnetic-field theory, the parameter-setting range for a theoretical model is often not largely restricted. One representative theoretical model is the Walfisch-Bertoni (W-B) model [Walfisch et al., 1988]. The W-B model is a widely used for over-rooftop propagation environments. It targets applications in the UHF band from 300 MHz to 3 GHz and introduces various mathematical approximations. Because of these approximations, millimeter-wave bands

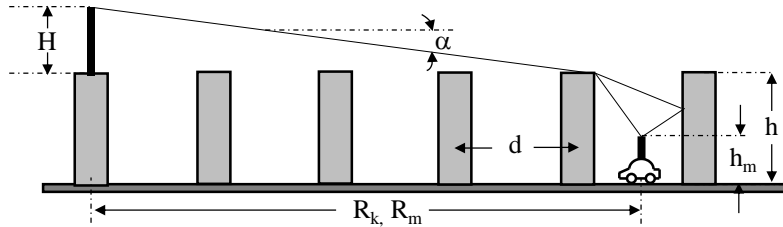
41 are out of the application range of the W-B model. In the current study, therefore, the applicable
 42 frequency range of the W-B model was extended to the millimeter wave band.

43 2 Walfisch-Bertoni Model and related models

44 2.1 Walfisch-Bertoni and related models

45 The model proposed by Walfisch and Bertoni is a physical model of propagation that takes
 46 place in urban environments. The geometry to explain the model is shown in Figure 1.

47



48

49 **Figure 1.** Considered situation and geometry of Walfisch-Bertoni model

50 In the model, α is the grazing angle (in units of radians) of a radio wave incident on one building
 51 of a row of buildings, R_k and R_m are horizontal distances in units of kilometers and meters,
 52 respectively, H is the height of the transmitting antenna from the building-rooftop level, d is the
 53 center-to-center spacing of the row of buildings, h is building height, and h_m is the height of the
 54 receiving antenna from ground level. In the W-B model, it is assumed that all of the building lows
 55 are of the same height, and the lows of buildings are replaced by a half screens. Using these
 56 parameters, the W-B model is formulated as follows:

57
$$L = L_f + L_{rts} + L_{msd}$$

58
$$L_f = 32.4 + 20 \log_{10}(f_{MHz}) + 20 \log_{10}(R_k)$$

59
$$L_{msd} = 68.9 - 9 \log_{10}(f_{MHz}) - 9 \log_{10}(d) + 18 \log_{10}(R_k) - 18 \log_{10}(H)$$

 60
$$- 18 \log_{10} \left[1 - \frac{R_k^2}{17H} \right]$$

61
$$L_{rts} = -8.8 + 10 \log_{10}(f_{MHz}) + 5 \log_{10} \left[\left(\frac{d}{2} \right)^2 + (h - h_m)^2 \right] + 20 \log_{10} \left\{ \tan^{-1} \left[\frac{2(h - h_m)}{d} \right] \right\}$$

62 where f_{MHz} is the frequency in MHz.

63 As shown above, this W-B model is composed of three components. The first component
 64 is free-space path loss, L_f , the second is path loss associated with diffraction down to street level,
 65 L_{rts} , and the third is path loss propagated over the rooftop by multiple diffraction past rows of
 66 buildings, L_{msd} . When this model was developed, the operating frequency bands of IMT systems
 67 were assumed as UHF bands. The applicable range of this model is therefore from 300 MHz to 3
 68 GHz in terms operating frequency and from 1 to 20 km in terms of propagation distance.

69 Based on the W-B model, several related models have been developed. For example, the COST
 70 231 Walfisch-Ikegami (W-I) model [Correia, 2009] basically follows the W-B model, but the

71 term L_{rts} is replaced by the model proposed by Ikegami, et al. [Ikegami et al., 1991]. When a base
72 station is placed above a roof top, the model is re-organized as follows:

$$73 \quad L = L_f + L_{rts} + L_{msd}$$

$$74 \quad L_f = 32.4 + 20 \log_{10}(f_{MHz}) + 20 \log_{10}(R_k)$$

$$75 \quad L_{rts} = -16.9 - 10 \log_{10}(w_s) + 10 \log_{10}(f_{MHz}) + 20 \log_{10}(h - h_m) + L_{ori}$$

$$76 \quad L_{msd} = -18 \log_{10}(H + 1) + 54 + 18 \log_{10}(R_k) + \left[-4 + 0.7 \left(\frac{f_{MHz}}{925} - 1 \right) \right] \log_{10}(f_{MHz})$$

$$77 \quad \quad \quad - 9 \log_{10}(d)$$

$$78 \quad L_{ori} = \begin{cases} -10.0 + 0.354\phi \\ 2.5 + 0.075(\phi - 35) \\ 4.0 - 0.114(\phi - 55) \end{cases}$$

79 where w_s is street width and ϕ is angle of signal arrival relative to the street axis.

80 The applicable range of the W-I model is from 800 MHz to 2 GHz in terms of operating
81 frequency and from 0.02 to 5 km in terms of propagation distance. The major difference between
82 the W-I and W-B models is in term L_{msd} . In the case of the W-B model, L_{msd} is derived theoretically,
83 while in the case of the W-I model, it is derived empirically on the basis of the W-B model. The
84 W-I model is widely adopted as an international standardized model [ITU-RP1411, 2019], and a
85 number of extensions to it have been presented.

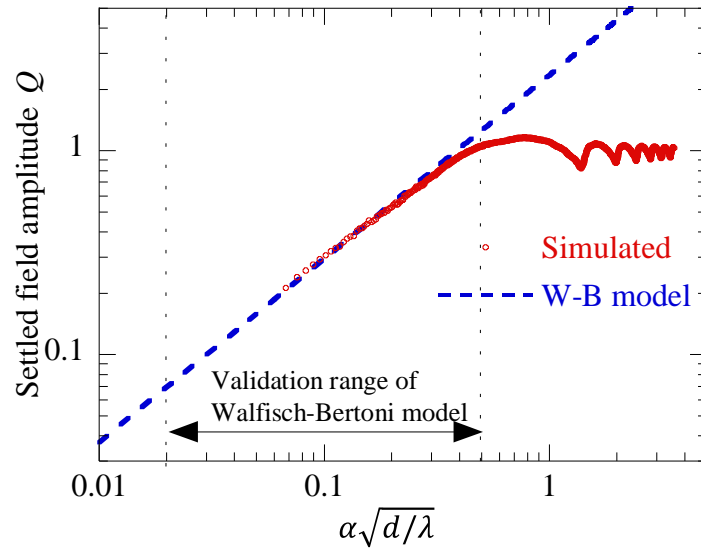
86 2.2 Problems with current models

87 When the W-B model was developed, some assumptions and approximations were applied.
88 Among them, assuming the same applicable range of operating frequency and propagation distance
89 when attempting to extend the model to higher frequency bands make is a critical problem.

90 Dependence of settled field amplitude Q [Walfisch et al., 1988] on parameter $\alpha\sqrt{d/\lambda}$ is
91 plotted in Figure 2. Red circles represent simulated values based on plane-wave diffraction by a
92 series of half screens. In the W-B model, it is assumed that the height of the base-station antenna
93 is 40 m, the distance to the mobile device is in the range 1 to 20 km, and a typical value of d is 40
94 m. Under these assumptions, the range of $\alpha\sqrt{d/\lambda}$ is from 0.02 to 0.5 for $f_{MHz} = 1$ GHz. In this
95 range, simulated settled field amplitude Q can be regarded as a straight line. Therefore, the curve
96 predicted with the W-B model is approximated as the blue dashed line in the figure. On the
97 contrary, the range of $\alpha\sqrt{d/\lambda}$ frequently exceeds 1.0 at frequency above the UHF band, such as
98 the millimeter-wave band. Moreover, α becomes large when distance R_k within 1 km (which is an
99 important area for IMT services on high-frequency bands). Even in this case, range of settled field
100 amplitude Q frequently exceeds 1.0. This means power is amplified while a signal is propagating
101 over multiple rooftops.

102 L_{msd} and L_{rts} calculated by the W-B model are shown in Figure 3. Parameters used in this
103 calculation are listed in Table 1. This figure shows that L_{rts} is a constant value regardless of
104 distance, and L_{msd} is increased with increasing distance R_k . On the contrary, L_{msd} has a positive
105 value above 500 m, but becomes negative below 500 m. This result implies travelling waves are
106 amplified below 500 m while propagating over multiple rooftop; however, realistically, such
107 amplification cannot happen.

108



109

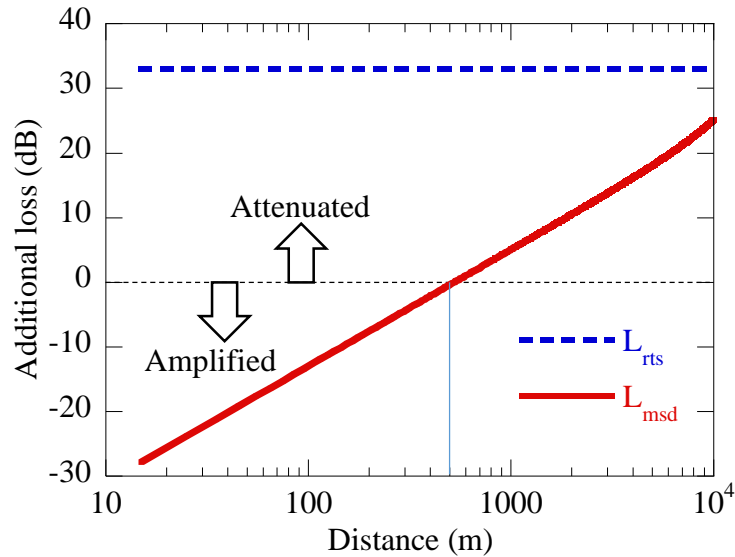
110

Figure 2. Dependence of settled field amplitude Q and parameter $\alpha\sqrt{d/\lambda}$

111

Table 1. Parameters for simulation

Simulation parameters	Value
f_M	1.0 GHz
H	25 m
h	15 m
h_m	1.5 m
d	20 m



112

113

Figure 3. Additional losses of L_{msd} and L_{rts}

114

115

116

117

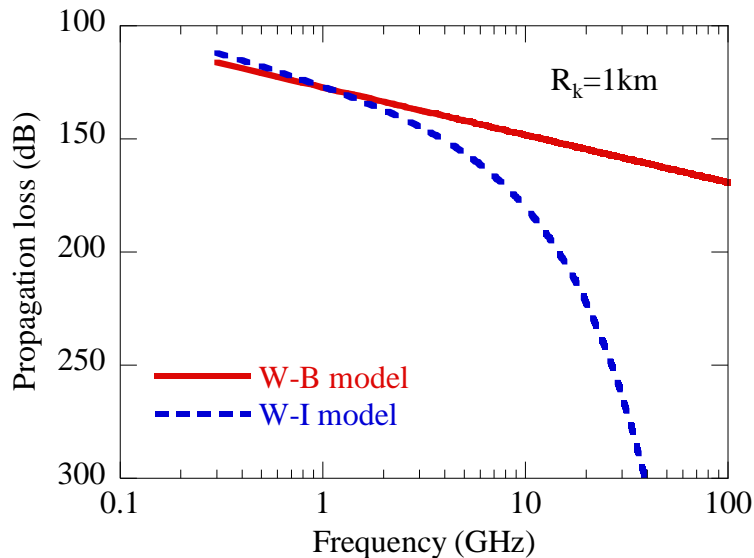
118

119

120

121

Predicted propagation loss by the W-B and W-I models at $R_k=1$ km is plotted in shows Figure 4. The horizontal axis represents frequency in unit of GHz. As shown in this figure, propagation loss in the case of the of W-B model increases linearly with increasing frequency. In contrast, propagation loss in the case of the W-I model increases greatly as frequency increases to an unrealistic level. This difference is due to differences in L_{msd} for both models. It is therefore concluded that a modeling approach based on the W-I model is not suitable for extending the frequency range. Accordingly, extending the frequency range by taking the approach based on the W-B model was investigated.



122

123

124

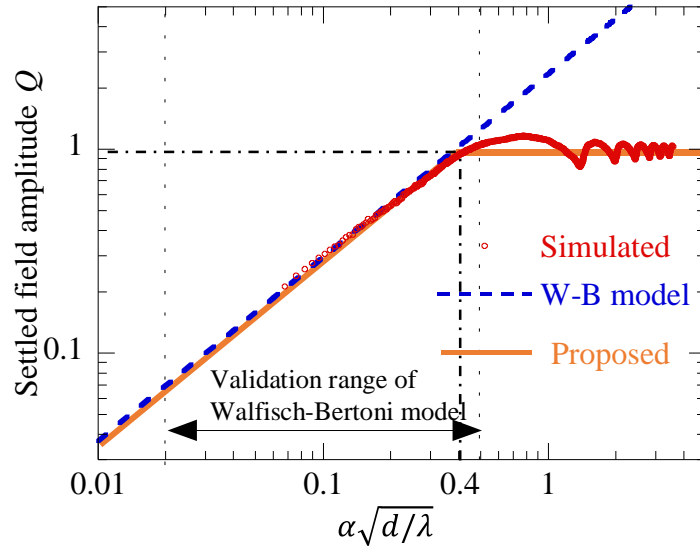
125

Figure 4. Examples of predicted results of W-B model and W-I model

126 **3 Modified W-B model to cover high-frequency bands**

127 3.1 Re-modeling of over-rooftop path

128 As described in Section 2.2, the original equation to derive L_{msd} has a problem in regard
 129 to covering high-frequency bands. The problem is that settled field amplitude Q exceeds 1.0
 130 from a certain region. Therefore, to solve that problem, it is proposed to divide the section into a
 131 region where settled field amplitude Q does not exceed 1.0 and a region where Q exceeds 1.0,
 132 and original equation is applied to the former region, and 1.0 is applied to the latter region. The
 133 modified model is characterized by the orange line shown in Figure 5



134

135 **Figure 5.** Characteristics of proposed and conventional models

136 The characteristics of the proposed and conventional models (expressed in units of dB) are given
 137 as follows:

138 L_{msd}

$$139 = \begin{cases} 16.8 + 20 \log_{10}(R_m) - 20 \log_{10}(H) - 10 \log_{10}(f_{MHz}) - 10 \log_{10}(d) & \text{for } \alpha \sqrt{\frac{d}{\lambda}} < 0.4 \\ 0 & \text{for } \alpha \sqrt{\frac{d}{\lambda}} \geq 0.4 \end{cases}$$

140 Here, some terms in original equation for L_{msd} have been deleted for simplification of equation.

141 3.2 Introduction of slant path

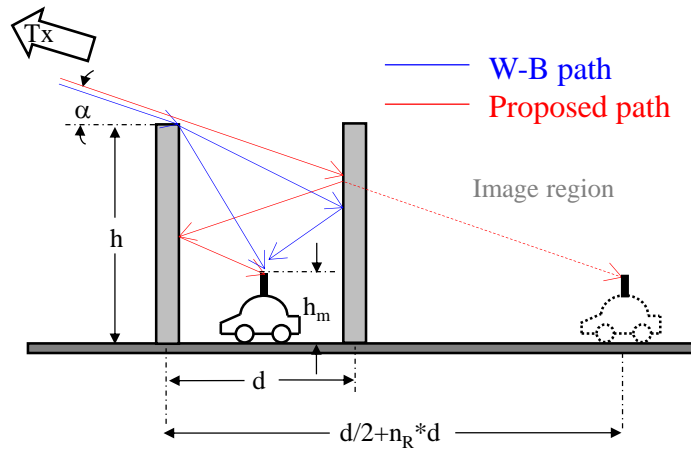
142 Actually, horizontal distance and actual propagation distance start to differ as the distance
 143 becomes shorter because of the difference in antenna height. For this reason, slant path rather than
 144 horizontal path has to be introduced. The equation for deriving L_f is therefore slightly modified as
 145 follows:

146 $L_f = -27.6 + 20 \log_{10}(f_{MHz}) + 20 \log_{10} \left[\sqrt{(R_m + d/2)^2 + (H + h - h_m)^2} \right]$

147 Here, variable of horizontal distance has been changed from R_k (in units of kilometers) to R_m (in
 148 units of meters).

149 3.3 Modeling of multiple reflections between buildings

150 A method for evaluating height-variation characteristics of propagation loss for fixed
 151 wireless access systems has been proposed [Kita et al., 2007]. In that study, it was revealed that
 152 propagation loss of multiple reflection waves from neighboring buildings is smaller than
 153 diffraction loss under some situation. Especially, multiple-reflection loss sometimes becomes
 154 smaller than diffraction loss in the high frequency band because diffraction loss increases with
 155 increasing frequency. Therefore, multiple reflection paths have to be considered for improving
 156 prediction accuracy of propagation loss.



157
 158 **Figure 6.** Considered propagation paths around the receiver and in the image region

159 When a receiving station with height h_m is located at the center of building spacing d as
 160 shown in Fig. 6, the number of inter-building reflections, n_R , can be derived from image region as
 161 follows:

$$162 \frac{H}{R_m} \leq \frac{h - h_m}{d/2 + n_R d}$$

163 When reflection loss per wall surface is L_r , additional loss L_{mr} due to multiple reflections between
 164 buildings can be calculated as follows:

$$167 L_{mr} = n_R L_R \leq \frac{2(h - h_m)R_m - dH}{2dH} L_r$$

165 Actually, number of reflections is an integer, so n_R should also be an integer. However, in this
 166 paper, it is defined that additional loss is calculated by using the right term of the above equation.

168 3.4 Summary of proposed model

169 To summarize the model introduced in Sections 3.1 to 3.3, the W-B model is modified to
 170 cover high-frequency bands as follows:

$$171 L = L_f + L_{msd} + \min(L_{mr}, L_{rts})$$

$$172 L_f = -27.6 + 20 \log_{10}(f_{MHz}) + 20 \log_{10} \left[\sqrt{(R_m + d/2)^2 + (H + h - h_m)^2} \right]$$

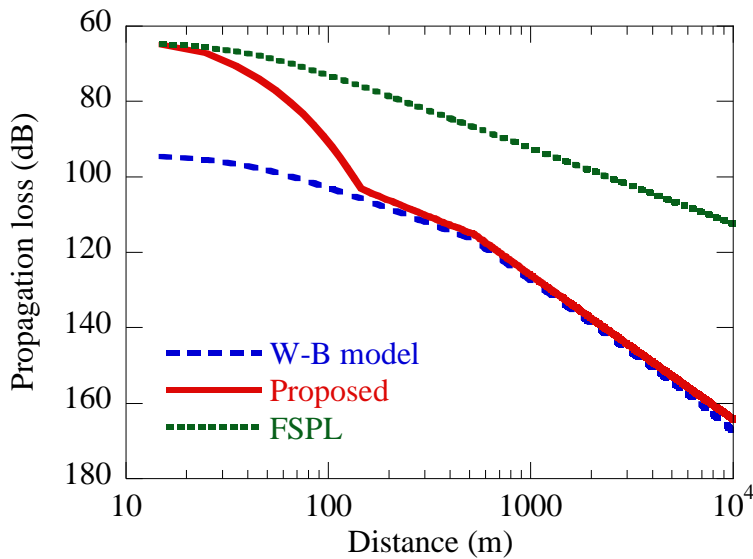
$$L_{msd} = \begin{cases} 16.8 + 20 \log_{10}(R_m) - 20 \log_{10}(H) - 10 \log_{10}(f_{MHz}) - 10 \log_{10}(d) & \text{for } \alpha \sqrt{\frac{d}{\lambda}} < 0.4 \\ 0 & \text{for } \alpha \sqrt{\frac{d}{\lambda}} \geq 0.4 \end{cases}$$

$$L_{rts} = -11.5 + 10 \log_{10}(f_{MHz}) + 5 \log_{10} \left[\left(\frac{d}{2} \right)^2 + (h - h_m)^2 \right] + 20 \log_{10} \left\{ \tan^{-1} \left[\frac{2(h - h_m)}{d} \right] - \alpha \right\}$$

$$L_{mr} = \frac{2(h - h_m)R_m - dH}{2dH} \times L_r$$

$$\alpha = \tan^{-1} \left(\frac{H}{R_m} \right)$$

An example of the prediction results given by the modified W-B model is shown in Figure 7. The parameters used in this simulation are identical to the values listed in Table 1. Difference between the proposed and original W-B models can be found within 200 m.



182
183 **Figure 7.** Examples of prediction

184 **4 Validation of proposed model by measurement**

185 4.1 Measurement environment and parameters

186 To validate the proposed model, propagation loss was measured in Tokyo, Japan. Measured
187 frequency bands were 2.2, 5.2, and 26.4 GHz with continuous waves. Measurement parameters
188 and environmental parameters are summarized in Table 2. The base station was set on the rooftop

189 of a building with height of 41.0 m from the ground. The antenna height was 1.5 m from the
190 rooftop, so the top of the antenna was 42.5 m from the ground. A receiver and data logger were
191 set on a measurement vehicle moving at approximately 30 km/h along a road of a predetermined
192 route. A receiving antenna was installed on the roof of the vehicle at a height of 2.7 m from the
193 ground. The antenna's radiation pattern was omni-directional in the horizontal plane for both the
194 transmitter and receiver.

195 A view from the base station to the measurement area is shown in Figure 8, and the locations
196 of the base station and measurement area are shown in Figure 9. Most of the buildings in the
197 measurement area are detached houses. The average building heights along the main roads that
198 cross from left to right and from top to bottom near the base station are higher than those in other
199 areas. However, in consideration of the total number of buildings in the measurement area, the
200 number of buildings along the main roads is small. Average building height of the measurement
201 area is therefore 8.3 m. Average building space is 14.2 m; however, the value of road orientation
202 which is an angle between the incident wave and street at which the measurement took place varies.
203 Accordingly, in the calculation of propagation loss, road orientation of 45 degrees (which is the
204 expected value) was assumed for deriving d . These environmental parameters were automatically
205 calculated by using our geographic information system.

206 Measured distance from the base station was from 30 to 1400 m, and total running distance
207 during the measurement was 23.6 km. However, due to the shielding effect of the rooftop surface
208 on which the base-station antenna was installed and the vertical radiation pattern of antenna,
209 measurement data acquired within a distance of 100 m were neglected. Measurement data were
210 gathered and averaged over 10-m intervals.



211

212

Figure 8. View from base station to measurement area



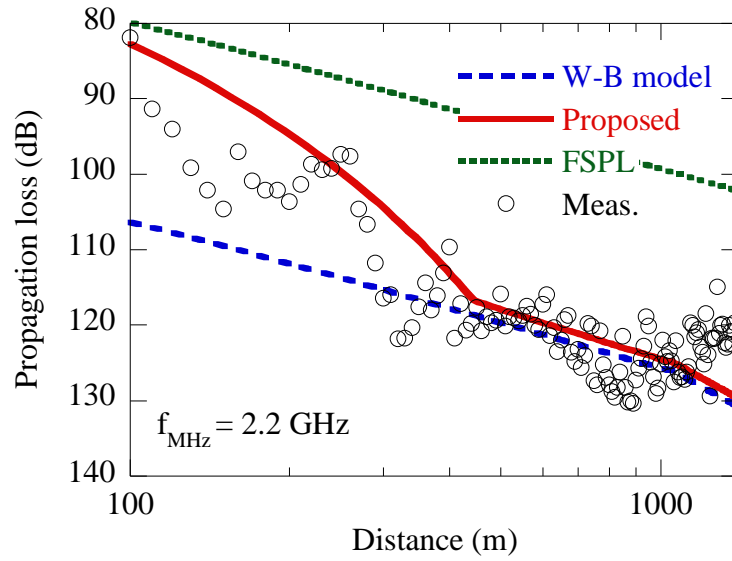
Figure 9. Locations of base station and measurement area

Table 2. Measurement condition and environmental parameters

Measurement parameters	Value
Frequency	2.2, 5.2, 26.4 GHz
Tx height	42.5 m
Rx height	2.7 m
Average building height	8.3 m
Average building spacing	14.2 m

4.2 Validation results

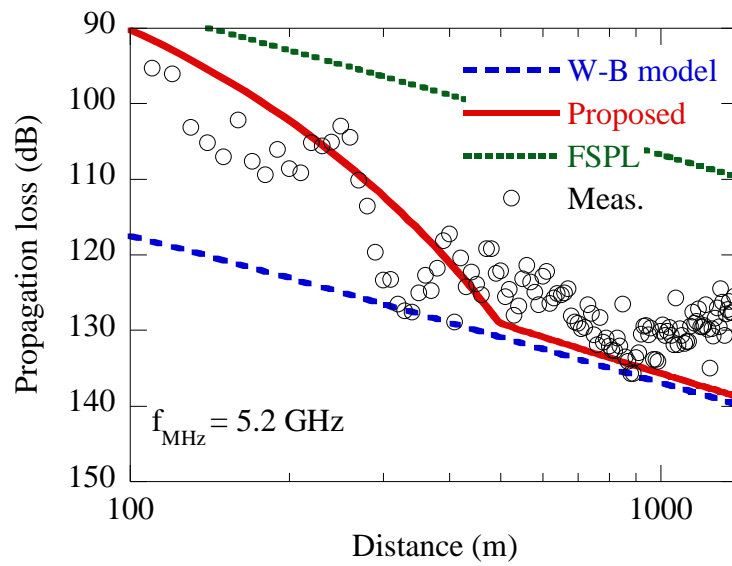
The measurement results and prediction results are compared in Figures 10, 11, and 12 for frequencies of 2.2, 5.2, and 26.4 GHz, respectively. Green dotted lines represent free-space path loss (FSPL), blue breaking lines shows results predicted by the W-B model, the red solid shows results predicted by the proposed model, and black circles show measurements. In this validation, L_r was set to 8 dB. These figures show that the prediction by the W-B model overestimate propagation loss. Especially, prediction error by the W-B model increases with decreasing distance. On the other hand, predicted propagation loss by the proposed model agreement well with the measurements for all frequency bands. Root mean square errors (RMSEs) of the W-B model are 6.5 dB for 2.2 GHz, 9.9 dB for 5.2 GHz, and 5.0 dB for 26.4 GHz, and RMSEs of the proposed model are 5.8 dB for 2.2 GHz, 6.6 dB for 5.2 GHz, and 3.3 dB for 26.4 GHz. Especially, in the distance range from 100 to 1000 m (which is the extended distance range for the proposed model), RMSEs of the W-B model are 6.5 dB for 2.2 GHz, 10.0 dB for 5.2 GHz, and 12.8 dB for 26.4 GHz, and RMSEs of the proposed model are 5.8 dB for 2.2 GHz, 5.6 dB for 5.2 GHz, and 7.7 dB for 26.4 GHz.



231

232

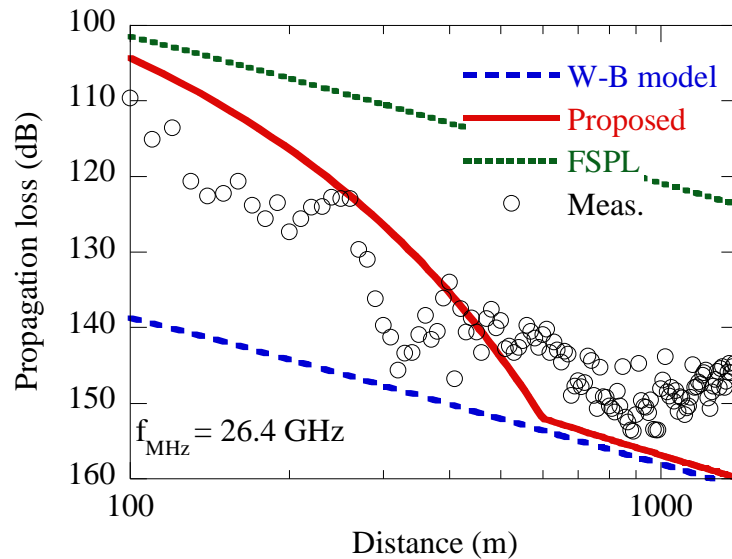
Figure 10. Measurement results and prediction results for 2.2 GHz



233

234

Figure 11. Measurement results and prediction results for 5.2 GHz



235

236

Figure 12. Measurement results and prediction results for 26.4 GHz

237 5 Conclusions

238 High-frequency bands, such as the millimeter wave band, are planned to be allocated to
 239 5G-and-beyond systems. To evaluate interference and design communication areas, a propagation
 240 model for these frequency bands has to be developed. To construct a theoretical propagation model
 241 that can estimate propagation loss in high-frequency bands, problems with the original Walfisch-
 242 Bertoni model (which is a representative theoretical model) are pointed out. The original W-B
 243 model was modified to extend it to higher frequency bands by three additions: (i) re-modeling over
 244 a rooftop path, (ii) introducing a slant path, and (iii) modeling of multiple reflections between
 245 buildings. To validate the proposed model, predicted propagation loss was compared with
 246 measurement propagation loss for frequencies in the range of 2.2 GHz to 26.4 GHz. The results of
 247 the comparison show that the propagation loss predicted by the proposed model agreement well
 248 with the measurement results for all measured frequency bands.

249 Acknowledgements

250 Datasets for this research are included in supplementary information file.

251 References

- 252 (ITU-RM2410, 2017) ITU-R Rep. M.2410-0 (2017), Minimum requirements related to technical
 253 performance for IMT-2020 radio interface(s). *ITU*, Geneva, Switzerland. 2017.
- 254 (WRC, 2020) Final Acts WRC-19 (2020), [https://www.itu.int/dms_pub/itu-r/opb/act/R-ACT-](https://www.itu.int/dms_pub/itu-r/opb/act/R-ACT-WRC.14-2019-PDF-E.pdf)
 255 [WRC.14-2019-PDF-E.pdf](https://www.itu.int/dms_pub/itu-r/opb/act/R-ACT-WRC.14-2019-PDF-E.pdf).
- 256 (DOCOMO, 2020) NTT DOCOMO (2020), 5G Evolution and 6G.
 257 [https://www.nttdocomo.co.jp/english/binary/pdf/corporate/technology/whitepaper_6g/DOCOMO](https://www.nttdocomo.co.jp/english/binary/pdf/corporate/technology/whitepaper_6g/DOCOMO_6G_White_PaperEN_20200124.pdf)
 258 [_6G_White_PaperEN_20200124.pdf](https://www.nttdocomo.co.jp/english/binary/pdf/corporate/technology/whitepaper_6g/DOCOMO_6G_White_PaperEN_20200124.pdf).

- 259 (Latva-aho et al., 2019) Latva-aho, M., & Leppanen, K., (2019), Key Drivers and Research
260 Challenges for 6G Ubiquitous Wireless Intelligence.
261 <http://jultika.oulu.fi/files/isbn9789526223544.pdf>.
- 262 (Sasaki et al., 2015) Sasaki, M., & Yamada, W., & Sugiyama, T., & Imai, T. (2015), Path Loss
263 Variation Characteristics at 26GHz Band in Street Microcell Environment. *IEICE*
264 *TRANSACTIONS on Communications* Vol. E98-B No. 5 pp. 783-789. doi:
265 10.1587/transcom.E98.B.783
- 266 (ITU-RM2412, 2017) ITU-R Rep. M.2412-0 (2017), Guidelines for evaluation of radio interface
267 technologies for IMT-2020. *ITU*, Geneva, Switzerland. 2017.
- 268 (Salous et al., 2020) Salous, S., Lee, J., Kim, M. D., Sasaki, M., Yamada, W., Raimundo, X.,
269 Cheema, A. A., Radio propagation measurements and modeling for standardization of the site
270 general path loss model in International Telecommunications Union recommendations for 5G
271 wireless networks. *Radio Science*, Vol. 55, Issue 1, January 2020. doi: 10.1029/2019RS006924
- 272 (Walfisch et al., 1988) Walfisch, J., & Bertoni, H. L. (1988), A Theoretical model of UHF
273 propagation in urban environments. *IEEE Trans. Antennas Propagat.*, vol. 36, 1988, 1788-1796.
274 doi: 10.1109/8.14401
- 275 (Correia, 2009) Correia, L. M. (2009), A view of the COST 231-Bertoni-Ikegami model. *3rd*
276 *European Conference on Antennas and Propagation*. EuCAP 2009. Berlin. March 2009.
- 277 (Ikegami et al., 1991) Ikegami, F., & Takeuchi, T., & Yoshida, S. (1991), Theoretical prediction
278 of mean field strength for Urban Mobile Radio. *IEEE Trans. Antennas Propagat.*, Vol. 39, No. 3,
279 1991, 299-302. doi: 10.1109/8.76325
- 280 (ITU-RP1411, 2019) ITU-R Rec. P.1411-10 (2019), Propagation data and prediction methods for
281 the planning of short-range outdoor radiocommunication systems and radio local area networks in
282 the frequency range 300 MHz to 100 GHz. *ITU*, Geneva, Switzerland. 2019.
- 283 (Kita et al., 2007) Kita, N., & Yamada, W., & Sato, A. (2007), New Method for Evaluating Height
284 Gain at Subscriber Station for Wireless Access Systems in Microwave Band. *IEICE*
285 *TRANSACTIONS on Communications* Vol. E90-B No. 10 2903-2914. doi:
286 10.1093/ietcom/e90-b.10.2903

Supporting information

Measurement data used in Section 4.2 are listed as follows:

Distance (m)	Propagation loss		
	2.2 GHz	5.2 GHz	26.4 GHz
100	81.942	88.521	109.6
110	91.393	95.281	115.06
120	94.046	96.09	113.59
130	99.199	103.13	120.66
140	102.19	105.19	122.59
150	104.65	107.03	122.21
160	97.098	102.2	120.65
170	100.96	107.69	123.84
180	102.11	109.38	125.6
190	102.15	106.06	123.5
200	103.62	108.61	127.37
210	101.38	109.19	125.59
220	98.748	105.16	124.12
230	99.428	105.65	124.05
240	99.243	105.1	122.8
250	97.412	103	122.98
260	97.622	104.48	122.95
270	104.61	110.15	129.69
280	106.65	113.58	131
290	111.75	119.65	136.16
300	116.45	123.36	139.7
310	116.04	123.32	141.27
320	121.82	126.52	145.6
330	121.79	127.41	143.47
340	120.33	127.58	143.33
350	117.58	125.08	140.93
360	114.46	122.76	138.4
370	118.06	124.78	141.56
380	116.07	121.82	140.51
390	113.09	118.11	136.08
400	109.66	117.31	134.04
410	121.78	128.96	146.75
420	117.13	120.47	137.48

430	120.69	124.21	140.64
440	119.8	122.28	138.77
450	117.69	123.9	140.57
460	120.76	125.33	143.32
470	118.92	119.19	138.8
480	119.7	119.23	137.6
490	119.34	122.53	140.05
500	115.95	122.13	139.06
510	120.14	125.57	142.84
520	118.93	124.57	142.5
530	119.1	128.02	143.32
540	119.47	126.81	142.58
550	118.71	123.17	141.75
560	117.5	121.47	139.69
570	118.55	123.68	140.55
580	120.07	124.96	141.45
590	120.57	126.64	142.6
600	117.23	122.86	140.93
610	115.97	122.24	140.28
620	121.39	126.42	143.31
630	120.36	125.79	141.88
640	123.52	125.12	142.98
650	122.05	125.26	144.6
660	119.3	125.04	143.21
670	118.72	124.54	143.51
680	123.62	128.1	149
690	124.82	128.92	147.72
700	123.25	129.14	147.02
710	125.66	129.79	147.82
720	124	129.68	147.32
730	119.79	126.59	143.81
740	120.2	127.78	144.35
750	127.45	130.62	148.95
760	127.87	131.93	150.72
770	120.78	128.28	145.31
780	125.32	131.55	149.16
790	126.92	131.09	149.26
800	127.91	132.12	150.37
810	128.81	132.59	150.71

820	129.59	132.71	151.22
830	128.24	131.09	148.46
840	126.21	132.12	150.41
850	121.49	126.54	145.15
860	128.32	133.52	151.93
870	130.19	134.09	152.48
880	130.04	135.73	153.54
890	130.39	135.7	153.75
900	127.29	133.63	151.57
910	125.69	132.96	144.72
920	124.48	130.52	149.66
930	122.82	129.4	150.49
940	118.94	129.38	150.62
950	120.14	130.61	151.24
960	124.91	129.71	149.61
970	126.84	133.88	153.51
980	129.08	133.85	153.55
990	128.35	134.1	153.59
1000	125.18	130.18	148.11
1010	122.02	129.31	147
1020	124.2	130.72	143.9
1030	124.84	130.13	148.58
1040	123.47	129.61	149.08
1050	124.74	130.7	147.95
1060	127.55	131.93	149.77
1070	122.1	125.78	148.38
1080	126.2	131.96	151.07
1090	126.93	129.83	149.2
1100	126.86	130.75	149.33
1110	127.25	131.76	151.58
1120	126.24	131.48	150.65
1130	125.51	131.51	150.37
1140	119.74	129.49	149.25
1150	120.06	127.58	144.94
1160	121.61	129.08	147.89
1170	121.03	128.82	147.82
1180	120.65	127.19	147.21
1190	122.93	129.59	147.5
1200	123.59	129.51	146.37

1210	125.18	129.4	146.04
1220	118.52	126.58	145.64
1230	123.96	129.87	149.35
1240	129.39	135	150.76
1250	121.72	129.77	148.58
1260	121.82	130.76	147.72
1270	121.8	128.39	146.81
1280	114.95	127.05	145.81
1290	121.12	129.52	147.93
1300	120.1	124.51	145.48
1310	119.89	126.28	145.23
1320	122.34	130.75	147.94
1330	123.01	127.85	147.15
1340	122.58	127.25	145.95
1350	120.08	126.21	144.73
1360	120.87	127.7	145.98
1370	122.56	127.64	145.19
1380	119.72	125.47	144.73